AIP | Review of Scientific Instruments

New phase and amplitude high resolution pulse shaper

Antoine Monmayrant and Béatrice Chatel

Citation: Review of Scientific Instruments **75**, 2668 (2004); doi: 10.1063/1.1771492
View online: http://dx.doi.org/10.1063/1.1771492
View Table of Contents: http://scitation.aip.org/content/aip/journal/rsi/75/8?ver=pdfcov
Published by the AIP Publishing

New phase and amplitude high resolution pulse shaper

Antoine Monmayrant and Béatrice Chatel
Laboratoire Collisions, Agrégats et Réactivité (CNRS UMR 5589), IRSAMC Université Paul Sabatier, 31062 Toulouse, France

(Received 1 December 2003; accepted 13 April 2004; published 3 August 2004)

We present the first realization of a femtosecond pulse shaper in phase and amplitude using two liquid crystal devices with 640 pixels, leading to a wide temporal window around 25 ps at 800 nm. Several examples illustrate the high resolution of such device. The use of a folded zero dispersion line is also successfully demonstrated. © *2004 American Institute of Physics.*
[DOI: 10.1063/1.1771492]

I. INTRODUCTION

The generation of arbitrarily shaped optical waveforms is of great interest in a number of fields including coherent control,[1–3] compression of optical pulses,[4] and optical communications.[5] Most of these works were spurred by technological breakthroughs. These pulse shaping techniques have been recently reviewed in details.[6] Due to their ultrashort duration femtosecond pulses are not easily shaped in the time domain. Thanks to the Fourier transformation, the common way to synthesize them is in the spectral domain. The most usual device for both high fidelity and wide flexibility of shapes involves a pair of diffraction gratings and lenses arranged in a zero-dispersion line[7] with a pulse shaping mask at the Fourier plane. This mask which can be a liquid crystal spatial light modulator (LC-SLM),[8] acousto-optic modulator[9] or deformable mirror,[10] modulates the spectral phase and/or amplitude. Shaping without Fourier transform optics is also possible by using an actively controlled acousto-optic programmable filter.[11] Let us focus on the mask using LC-SLMs. Phase-only LC-SLM with 128 to 640 pixels are commercially available. To our knowledge, phase and amplitude modulation has only been demonstrated with 128 pixels or less, using in most cases dual-LC-SLM device from CRI (Cambridge Research & Instrumentation) company. In this article, we combine two 640-LC-SLMs from Jenoptik company with a highly dispersive zero-dispersion line to build a phase and amplitude pulse shaper (of 2×640 parameters). The main characteristic of this pulse shaper is a high spectral resolution in phase and amplitude corresponding to a wide temporal range. In the following, we first describe the experimental setup and the alignment procedure of the two LC-SLMs, then we present a few examples illustrating the capacity of such a pulse shaper. We also present an alternative scheme consisting on folding the 4f-line.

II. EXPERIMENTAL SETUP

Before describing the experimental setup, let us recall some basics concerning phase and amplitude modulation. As previously shown,[12] two LC-SLMs are needed. Let us consider the incoming field E_1 to be polarized along the x axis, z being the propagation axis. The LC molecules are aligned along the axis at $+45$ and -45 degrees in the $x-y$ plane. The x polarized contribution to E_2 of the outcoming field can be written as

$$E_{2x}(x) = E_1(x) \times \exp\left(i\frac{\phi_1(x)+\phi_2(x)}{2}\right)\cos\left(\frac{\phi_1(x)-\phi_2(x)}{2}\right), \quad (1)$$

where ϕ_1 and ϕ_2 are the voltage dependent birefringences of the first and the second LC-SLM array, respectively. So by using an output polarizer along the x axis, the output phase and amplitude can be set independently by controlling the sum and the difference of both LC-SLM birefringences, respectively. Moreover, the use of orthogonal polarizations on each LC-SLM limits multiple diffraction.[12] The LC-SLM (SLM-S 640/12) produced by Jenoptik company, possesses 640 pixels and has been described in Ref. 13 (stripes of $97\,\mu\text{m}\times 10$ mm separated by gaps of 3 μm). The birefringence of each pixel is controlled by a voltage with a dynamic range of 12 bits. The nonlinear relation between voltage, incident wavelength, and birefringence is carefully calibrated.[13] To avoid any Fabry-Perot effects as well as to reduce losses, the two outer surfaces of each LC-SLM have an antireflection coating on a broad spectral range. The two LC-SLMs are mechanically independent and the two mountings provided by Jenoptik company have been adapted to provide a distance of less than 1 mm between both LC-SLM. This distance is much smaller than the Rayleigh length which is equal to ca. 2 cm. This setup requires a micrometric control of 5 degrees of freedom for each LC-SLM (rotations around x, y, and z axis and translations along the x and z axis). Both LC-SLMs are prealigned on a common base plate using the following procedure.

A first LC-SLM is placed on the common base plate and illuminated by a He–Ne laser. The rotation angles around the x axis (horizontal transverse) and the y axis (vertical) are set by autocollimation of the reflected part of the He–Ne beam (accuracy 6 mrad). The rotation around the z axis (propagation axis) is set by looking at the diffraction pattern of the transmitted beam. This pattern should be horizontal for ver-

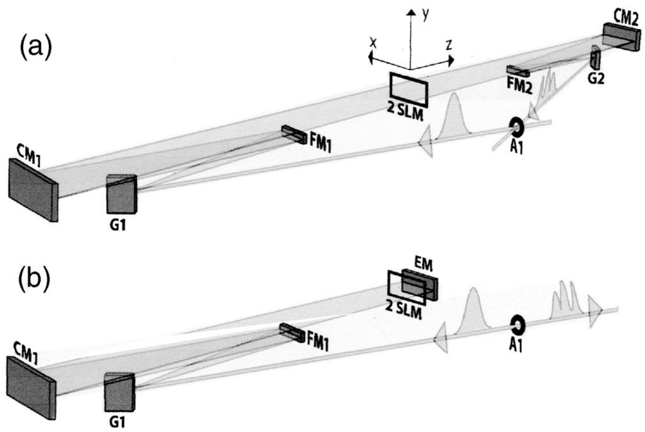

FIG. 1. (a) Usual setup, A1 is an alignment aperture for both input and output, FM1 and FM2 are plane folding mirrors and CM1 and CM2 are the cylindrical mirrors. Both LC-SLM are at the Fourier plane. (b) Half-line setup, an end mirror EM is placed just after the LC-SLM and the beam goes twice through the first half of the line.

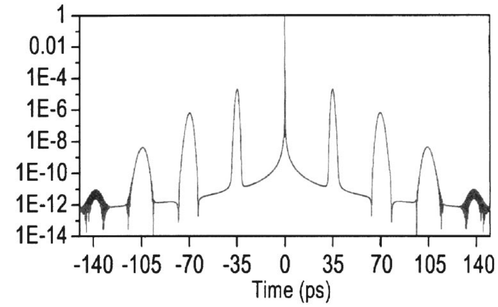

FIG. 2. Calculated replica due to the mask pixelization, taking the nonlinear dispersion into account. The delay between replica is 35 ps. The nonlinear dispersion broadens and attenuates the replica.

tical stripes. Then, the second LC-SLM is placed on the base plate, between the first LC-SLM and the laser. We apply exactly the same procedure to set all the rotational angles. The superposition of both diffraction patterns gives a matching of the z angles with an accuracy better than 2 mrad. For the translation along the x axis the He–Ne beam is expanded to cover all the LC-SLM and two x polarizers are inserted: one before the first LC-SLM, the other after the second LC-SLM. Therefore, the transmitted beam is given by Eq. (1). In the first LC-SLM we program a phase of π on the first 320 pixels and 0 on the others. In the second LC-SLM an inverted pattern is set: 0 on the first 320 pixels and π on the others. Thus, according to Eq. (1), the transmitted intensity $|E_{2x}(x)|^2$ is null if the lateral displacement between the two LC-SLM is null. If not, a bright stripe with a width equal to the displacement appears in the transmitted beam. The sensitivity of this alignement is of the order of the gap size. Once this prealignment is done, the base plate is inserted as a dual-LC-SLM in the zero-dispersion line without misalignment. Spectral pattern (as pulse sequences, amplitude hole) are also used to refine the alignment inside the zero dispersion line.

To avoid chromatic as well as off-axis aberrations, the setup reported in Fig. 1(a) is chosen. For sake of simplicity, the input and output polarizers and apertures are not represented. The alignment aperture A1 guarantees the symmetry of the line. A special care is taken to cancel the spatial chirp of the output beam. The two cylindrical mirrors have a focal length of 600 mm, the gold-coated gratings have 2000 lines/mm and the LC-SLM width in the Fourier plane is 64 mm. The central wavelength is set to 795 nm. These characteristics provide an average resolution of 0.06 nm/pixel corresponding to a spectral width of 38 nm. This spectral width is large enough to transmit the spectral pedestal width of our laser source [full width at half maximum (FWHM) of 10 nm]. The sagital beam FWHM in the Fourier plane (57 μm, corresponding to an input beam diameter of 2.3 mm) is roughly set to the width of a pixel.

As any shaper pixelized in the spectral domain, our shaper introduces temporal replica. In our case, these replica are separated by 35 ps and are especially broad and weak (see Fig. 2). This broadening of replica is due to the nonlinear dispersion in the masking plane.[14]

Therefore a particular procedure is used to calibrate this nonlinear dispersion. This time window of 35 ps is restricted down to 28 ps by the effect of the Gaussian envelope (due to the spatial beam profile in the masking plane[6]). By applying successively several linear phases regularly spaced in time, the maxima clearly reproduce this Gaussian envelope (Fig. 3). This FWHM in intensity of 28 ps corresponds to an input diameter beam of 2.3 mm. The Gaussian time window function significantly reduces the replica pulses.

The spatial-time coupling parameters in our pulse shaper is around 83 μm/ps which is quite small as compared to common devices (for example, 145 μm/ps as described in Ref. 15). To limit space–time coupling an aperture is placed on the output beam. For the examples given in the following, the output diameter is ca. 1 mm. Although the efficiencies of the gratings mainly limit the total energy throughput of the pulse shaper, the overall transmission in intensity of all the device is currently of 60% and the on–off ratio (degree of extinction) of 20 dB. The main limitation to this ratio is the gaps effect and by an appropriate compensation[12] we reach a ratio of nearly 30 dB.

In the following, a Kerr–Lens–Mode-locking Ti:sapphire oscillator which supplies 400 mW with a repetition rate of 80 MHz is used as the laser source. The central wavelength is 795 nm. The spectral FWHM is 10 nm and the temporal FWHM is 100 fs (assuming a Gaussian intensity profile). A

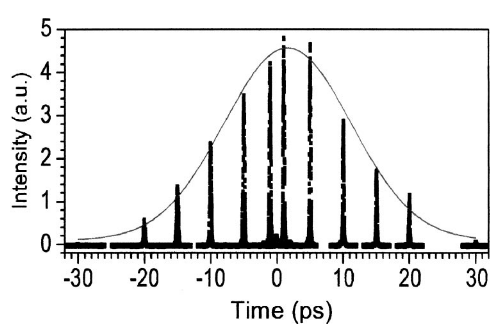

FIG. 3. Several experiments without compensation for different linear phases inducing a temporal shift and a constant amplitude (black dots). The desired shape is multiplied by a Gaussian envelope (gray line) because of the spatial profile in the masking plane.

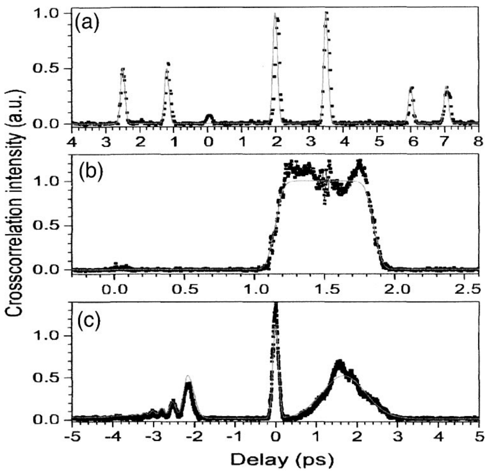

FIG. 4. Calculated (gray line) and experimental (black dots) wave forms. (a) Three pulses pairs with relative intensity of 2:3:1, (b) square pulse of 700 fs, and (c) three pulses with cubic phase (9×10^7 fs^3), no phase and quadratic phase (5×10^4 fs^2), respectively.

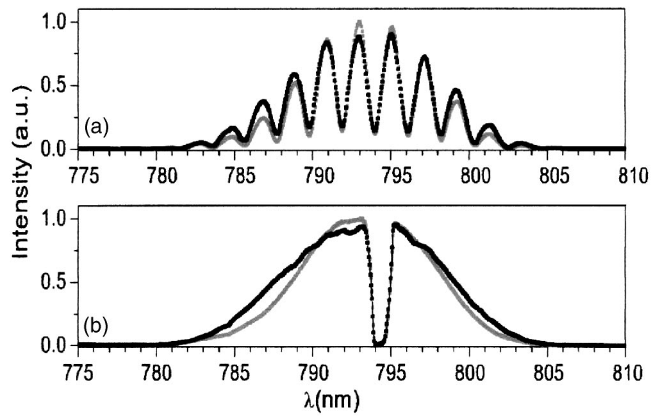

FIG. 5. Compared shapes for the usual setup (gray) and the folded line (black): (a) two pulses delayed by 1 ps, (b) spectral hole of 20 pixels ca. 1.2 nm centered in 794.3 nm.

fraction of the energy passes through the pulse shaper when the other part of the pulse is used as reference for the cross-correlation intensity measurement. Other nice results[16,17] using a conventional kHz system delivering 800 μJ–130 fs–1 kHz–795 nm pulses have been obtained thanks to the high damage threshold of 300 GW/cm^2.

III. RESULTS AND DISCUSSION

To illustrate the fine control on a wide time window allowed by our device, we choose some masking operations using amplitude and phase modulation.

Three examples are presented in Fig. 4: (a) three equal-amplitude pulses pairs with relative intensity 2:3:1, (b) a square pulse of 700 fs, and (c) three pulses with quadratic, no phase, and cubic phase. For each example, black dots correspond to the experimental result whereas the solid gray line is the analytical desired wave form. In all three cases, the agreement is excellent in both phase and amplitude over a large temporal window, whereas the analytical wave form does not take into account any limitations inherent in the LC-SLM. The effect of the gaps (replica at $t=0$) and the spatial profile (Gaussian temporal envelope) should be compensated in the applied mask. This can be done by an iterative procedure.[12] For the square pulse [Fig. 4(b)], the main defect is some ripples that are perfectly explained by the truncation of the spectrum. In these three examples, the gaps contribution at $t=0$ is not perfectly compensated. A better knowledge of the gaps behavior would allow an improvement of this compensation. Other examples using the same setup but with phase-only mask have been obtained. High quadratic phase, or pi-step have been successfully implemented in an atomic physics experiment.[16] According to the Nyquist's criteria, quadratic phase up to 6×10^5 fs^2 is easily synthesized without any temporal distorsion. Higher quadratic phase in the spectral domain are feasible (9×10^5 fs^2 has been demonstrated in Ref. 16) but the duration of the pulse increases more slowly than it should because of spectral narrowing. A phase varying as a function of $1/\Delta\lambda$ has also been successfully synthesized to compensate propagation effects in a dense vapor.[17]

To complete this study, a half-zero-dispersion line has been implemented by simply placing a mirror just after the dual LC-SLM [see Fig. 1(b)]. In this design, only half of the optical elements are used and the beam passes twice in the dual LC-SLM. This reduces the dynamic range of the voltage from 12 to 11 bits. However this reduces also the size of the device and its cost without reducing the resolution in the spectral domain. Moreover, by construction this setup provides a perfect symmetry of the zero-dispersion line which simplifies greatly the alignment procedure. The only precaution is to place the mirror in the Fourier plane and very close to the dual LC-SLM to limit misalignment effect. This condition is fulfilled thanks to the large Rayleigh length. In Fig. 5 two spectral features obtained with the half-line (black line) and the full-line (gray line) are compared. Figure 5(a) corresponds to two pulses delayed by 1 ps while Fig. 5(b) is a spectral hole of 20 pixels (ca. 1.2 nm) centered on 794.3 nm. The agreement is very good in both cases. Some small differences remain probably due to the change of the alignment in the spectrometer.

IV. DISCUSSION

We have presented the successful implementation of a phase and amplitude pulse shaper using a two 640 pixels LC-SLM. With the increased number of pixels and the high resolution zero-dispersion line, the manifold of accessible pulse modulations exceeds that of previous phase and amplitude devices. The device provides a wide window which can be very useful in many coherent control experiments.[16,17] The high threshold damage makes it suitable for high intensity applications. We have also shown that it is possible to considerably simplify the setup by folding the zero-dispersion line without reducing the spectral resolution. Finally the broad spectral range of LC-SLM working provides an excellent tool to extend high resolution phase and amplitude pulse shaping in the UV domain.[18]

ACKNOWLEDGMENTS

The authors sincerely acknowledge the technical staff for the built of the specified mechanical mounting of the double LC-SLM, Barbara Lamory for her work on the alignment procedure and W. Wohlleben (MPQ-Garching) for his help on the computer interface. We also thank the technical staff from the Jenoptik company, G. Stobrawa (IOQ-Jena), K. Nelson (MIT), and B. Girard (LCAR-IRSAMC) for fruitful discussions. This work has been financially supported by CNRS-Rég. Midi-Pyrénées-Ministère de la Recherche (CPER: "Spectroscopie ultime").

[1] A. Assion, T. Baumert, M. Bergt, T. Brixner, B. Kiefer, V. Seyfried, M. Strehle, and G. Gerber, Science **282**, 919 (1998).
[2] J. Degert, W. Wohlleben, B. Chatel, M. Motzkus, and B. Girard, Phys. Rev. Lett. **89**, 203003 (2002).
[3] J. L. Herek, W. Wohlleben, R. J. Cogdell, D. Zeidler, and M. Motzkus, Nature (London) **417**, 533 (2002).
[4] A. Efimov, M. D. Moores, B. Mei, J. L. Krause, C. W. Siders, and D. H. Reitze, Appl. Phys. B: Lasers Opt. **70**, S133 (2000).
[5] H. P. Sardesai, C. C. Chang, and A. M. Weiner, J. Lightwave Technol. **16**, 1953 (1998).
[6] A. M. Weiner, Rev. Sci. Instrum. **71**, 1929 (2000).
[7] O. E. Martinez, IEEE J. Quantum Electron. **QE-23**, 59 (1987).
[8] A. M. Weiner, J. P. Heritage, and E. M. Kirschner, J. Opt. Soc. Am. B **5**, 1563 (1988).
[9] M. A. Dugan, J. X. Tull, and W. S. Warren, J. Opt. Soc. Am. B **14**, 2348 (1997).
[10] E. Zeek, K. Maginnis, S. Backus, U. Russek, M. Murnane, G. Mourou, H. Kapteyn, and G. Vdovin, Opt. Lett. **24**, 493 (1999).
[11] F. Verluise, V. Laude, Z. Cheng, C. Spielmann, and P. Tournois, Opt. Lett. **25**, 575 (2000).
[12] M. M. Wefers and K. A. Nelson, J. Opt. Soc. Am. B **12**, 1343 (1995).
[13] G. Stobrawa, M. Hacker, T. Feurer, D. Zeidler, M. Motzkus, and F. Reichel, Appl. Phys. B: Lasers Opt. **B72**, 627 (2001).
[14] L. Wang and A. M. Weiner, Opt. Commun. **167**, 211 (1999).
[15] M. M. Wefers and K. A. Nelson, IEEE J. Quantum Electron. **32**, 161 (1996).
[16] W. Wohlleben, J. Degert, A. Monmayrant, B. Chatel, M. Motzkus, and B. Girard, Appl. Phys. B: Lasers Opt. (to be published).
[17] J. C. Delagnes, A. Monmayrant, P. Zahariev, B. Chatel, B. Girard, and M. A. Bouchene (unpublished).
[18] M. Hacker, T. Feurer, R. Sauerbrey, T. Lucza, and G. Szabo, J. Opt. Soc. Am. B **18**, 866 (2001).